

BOWED STRING SIMULATION USING A THERMAL FRICTION MODEL

J Woodhouse

Cambridge University Engineering Department

1. INTRODUCTION

Much of the special quality of the violin derives from the complex and subtle range of vibration behaviour of a string excited by bowing. In recent decades, understanding of this behaviour has advanced steadily. Progress has been made by the development of increasingly complete theoretical models of the bowing process, and by comparing simulations based on these models with observations of real bowed strings. As a result many features of bowed-string motion have been explained qualitatively, and to a certain extent quantitatively¹⁻⁷.

One ingredient of these models which has remained largely unquestioned since the earliest work is the description of the interfacial friction between bow and string. It has been conventional to assume that the frictional force is governed by the speed of relative sliding between bow and string. If experimental measurements are made of the coefficient of friction of a rosin-coated surface during steady sliding at different speeds, results are obtained like those shown in Fig. 1^{2,8}. Given results like these it is an easy step to suppose that during stick-slip oscillation, when the sliding speed is varying rapidly, the friction force is still governed solely by the instantaneous value of sliding speed according to the steady-sliding curve. However, there is no obvious physical reason why this should be true, and recent measurements have shown decisively that in fact it is not true^{8,9}. If the force f and sliding velocity v are measured during stick-slip motion with rosin at the interface, the results can be plotted in the f - v plane. What is found is a hysteresis loop. At the end of sticking the friction force is high, and as sliding begins the force falls rapidly. During the return to sticking, though, the force remains quite low.

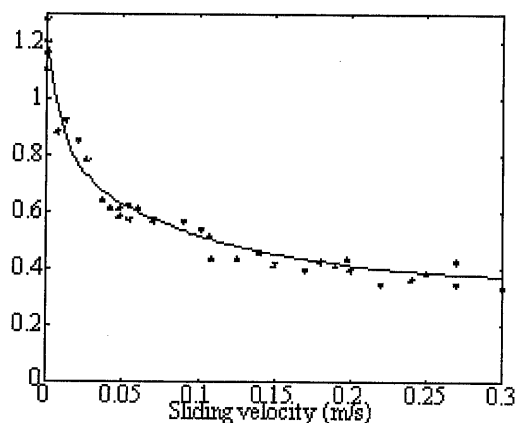


Figure 1: Friction coefficient as a function of sliding speed; measured (points) and curve fit (line)

A different friction law is needed to account for this behaviour. Based on a variety of evidence, it has been suggested⁸ that the simplest plausible model is obtained by supposing that the friction force during sliding does not depend directly on variations of sliding speed, but rather on variations of temperature in the interfacial rosin layer. Rosin is a brittle solid at room temperature, but it softens and undergoes a glass transition at temperatures not much higher than this. This implies that the mechanical behaviour will be sensitive to temperature in the range just above normal ambient: in particular the shear strength of a rosin layer will decrease as temperature increases. The behaviour shown in Fig. 1 is consistent with such a model: there is a monotonic relation between contact temperature and speed of steady sliding, which could account for the falling trend of the friction force with sliding speed.

A simple model based on this idea has been developed⁸, and used with some success to reproduce the results of the measurements. These first measurements were made, not with a bowed string, but with a vibrator which behaved approximately like a harmonic oscillator. Subsequently, similar measurements have been made using a bowed string⁹. These showed qualitatively similar behaviour: in particular they showed similar hysteresis behaviour in the f - v plane. It is thus natural to use the proposed thermal model of rosin friction to carry out bowed-string simulations to see whether it is capable of reproducing features of the observations. That is the task of this paper.

2. THE SIMULATION MODEL

2.1 The thermal friction model

In the steady-sliding measurement which produced the data of Fig. 1, the geometry of the contact was that of two crossed cylinders of perspex (PMMA) loaded together to give an approximately circular contact area. One of the cylinders was stationary, while the other moved across it carrying a layer of rosin. This rosin would be at ambient temperature on entry to the contact zone. As it moves into the contact zone frictional energy will heat the surface of the rosin layer, probably sufficiently that it sticks to the fixed cylinder. There would then be a layer of some thickness within which shearing motion takes place. This might be a relatively thick layer within which the deformation is best described as viscous flow, or it might be a thin interfacial layer better described by visco-plastic yielding of rosin in a semi-solid state. It was shown [8] that a model based on the latter possibility produced a more satisfactory match to the results of stick-slip measurements, and the same model will be used here.

The temperature at the sliding contact can be calculated by modelling the heat generation and transfer in the material surrounding the interface. The rate at which heat is generated at the contact is given by the product of the frictional force and the sliding velocity. This heat input is balanced by three effects: conduction into the two neighbouring solids, convection with the rosin as cold material flows into the contact region while heated material flows out, and absorption in the contact volume, changing its temperature. This model is suitable for time-stepping simulation once the time derivative is represented as a forward difference, and it is easily incorporated into the type of bowed-string simulation described in earlier references^{2,3,5,10}. The first task for this model, needed for calibration purposes, is to simulate the conditions of the steady-sliding experiment. This gives the contact temperature as a function of sliding speed, and once that is known the results for friction force shown in Fig. 1 can be converted into a function of temperature which can then be used in bowing simulations.

2.2 Bowed string simulation

Modelling of the dynamic behaviour of the string is subject to fewer uncertainties than the friction model. All the simulation results in this paper are based on modelling the best-understood musical string, a “Dominant” cello D string. For this particular string a reasonably complete set of calibration data is available, covering transverse vibration frequencies and damping factors, torsional frequencies and damping factors, and bending stiffness. Empirically, the transverse modes have, very approximately, constant Q factors for a wide range of overtones. The transverse string damping is simulated using the constant-Q reflection function described in an earlier work¹¹. Bending stiffness is also allowed for, using the stiff-string reflection function described earlier⁵. The torsional wavespeed at nominal string tension has been measured at 1060 m/s, and the first few torsional modes of the string have been shown to have constant Q factors of approximately 45¹¹. A suitable version of the constant-Q reflection function is used to simulate this behaviour. The position of the bowed point on the string is denoted, as usual, by the dimensionless quantity β , the fractional distance of the “bow” from the bridge. Results will be shown for a wide range of values of β , in order to plot “Schelleng diagrams”.

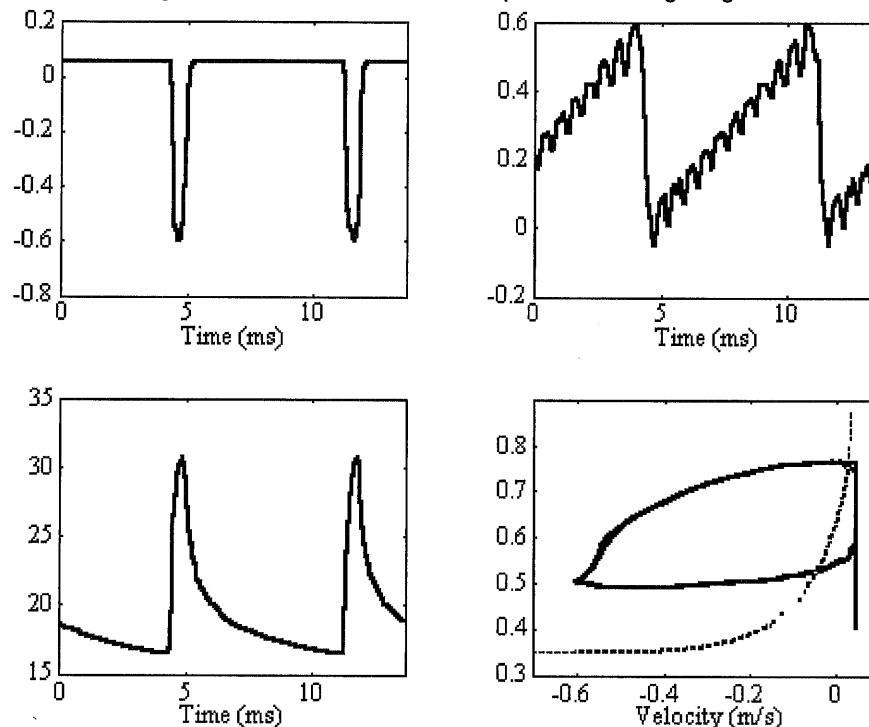


Figure 2. Simulated bowed-string waveforms using thermal friction model. (a) string surface velocity (m/s); (b) velocity wave from bow towards bridge (m/s); (c) temperature ($^{\circ}\text{C}$); (d) friction coefficient against surface velocity (solid), steady curve of Fig. 1 (dashed).

An example of the output from this simulation program is shown in Fig. 2. This shows the last two period-lengths after a simulation of length 0.4 s (i.e. 59 period-lengths at the nominal 147 Hz), the string having started at rest. It is reassuring to see that the new friction model has produced a version of the familiar Helmholtz motion (see e.g. refs. 1,2), characterised by a single episode of slipping per cycle (shown by the waveform of surface velocity in Fig. 2a) and an outgoing velocity wave which is a sawtooth wave (see Fig. 2b). Figure 2c shows the temperature variation at the contact associated with the vibration, and Figure 2d shows the path traced in the f - v plane by the results. A hysteresis loop is clearly visible, traversed in the anticlockwise direction as seen in measured results⁹.

For comparison, Figure 3 shows the results of a simulation using the identical string model and bowing parameters, but using the friction-curve model in place of the thermal model. This model

also predicts a Helmholtz motion under the assumed conditions, but the waveform details are quite different: the edges of the velocity pulse during slipping are steeper, and the amplitude of “Schelleng ripples”^{1,4} visible in the outgoing velocity waveform (Fig. 3b) is larger than with the thermal model. The $f-v$ plane (Fig. 3c) this time shows all points lying on the assumed friction curve, as expected. The “missing” portion of the friction curve, at low sliding speeds, corresponds to the portion which is leapfrogged by the jumps resulting from the Friedlander construction^{3,12}.

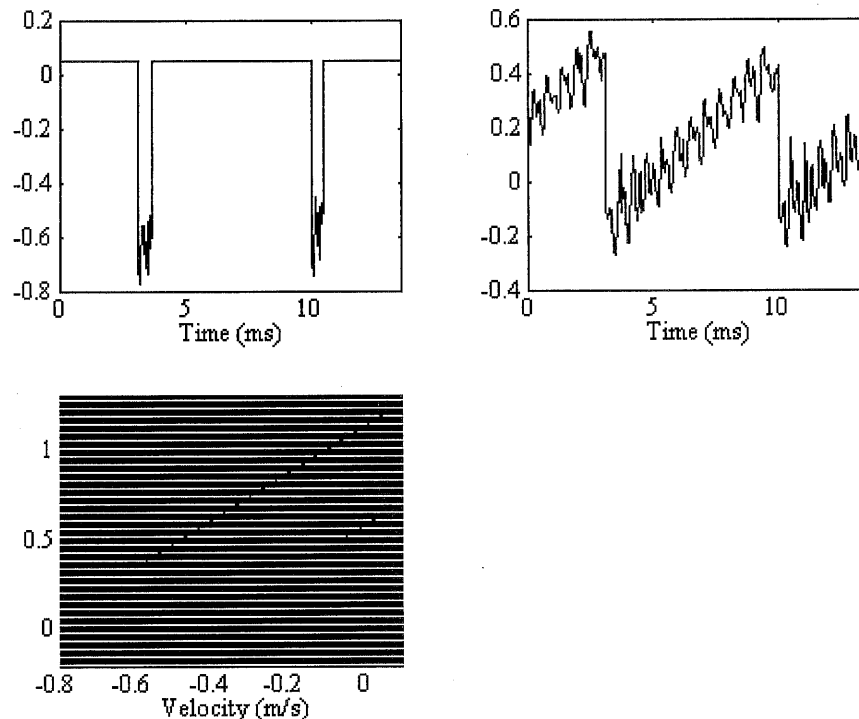


Figure 3. Simulated bowed-string waveforms using friction-curve model. (a) string surface velocity (m/s); (b) velocity wave from bow towards bridge (m/s); (c) friction coefficient against surface velocity (symbols), curve of Fig. 1 (dashed).

3. SCHELLENG DIAGRAMS

For a systematic comparison of the two friction models, it is necessary to compare the predictions over a range of parameter space rather than simply looking at individual cases. We choose here the “Schelleng diagram”. Schelleng¹ calculated formulae for the maximum and minimum bow forces between which the Helmholtz motion of the string is possible, and plotted the results in the plane of force against bowing position β . Schelleng’s calculations, and their extensions to more realistic string models⁶, are based explicitly on the friction-curve model, and it is natural to ask whether the thermal model predicts similar behaviour. The simulation programs were run for a grid of points covering the relevant range of this parameter plane. The points were chosen to be logarithmically spaced on both axes, since the standard Schelleng diagram is plotted on log-log axes to bring out the different power-law relations: Schelleng’s minimum bow force is proportional to β^{-2} , while his maximum force is proportional to β^{-1} .

Results are shown in Figure 4a for the thermal friction model assuming that the string starts at rest. Different plotted symbols denote the following outcomes: Helmholtz motion (square); multiple-slipping motion (x); decaying motion (dot); non-periodic raucous motion (+); ALF

(triangle); and periodic motion showing a Raman “higher type” such as S-motion (star). For the cases which eventually produced Helmholtz motion, the transient length was also computed, and is plotted in Figure 4b. Corresponding results computed with the friction-curve model using otherwise identical parameters are shown in Figure 5.

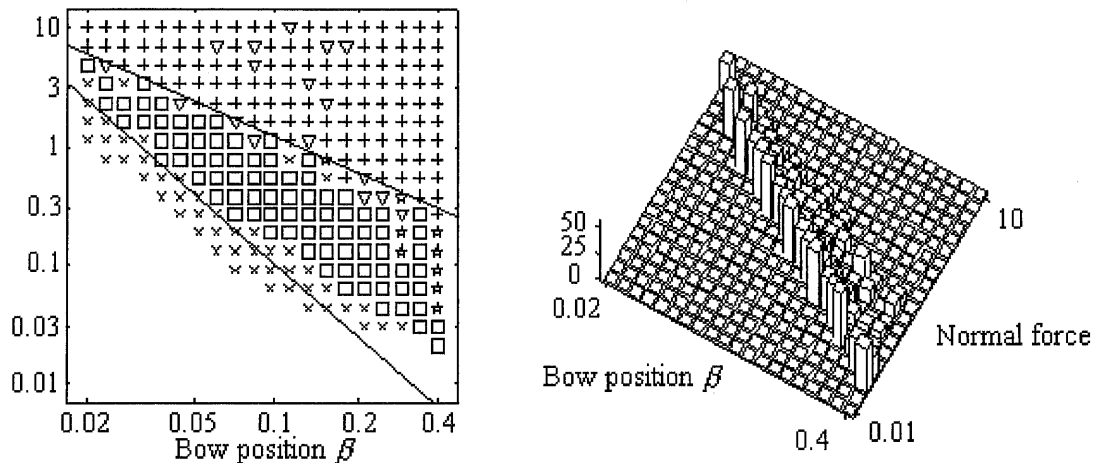


Figure 4. Results of transient bowing simulations using thermal friction model. (a) Schelleng diagram of normal force (N) versus bowing position; (b) transient length in periods.

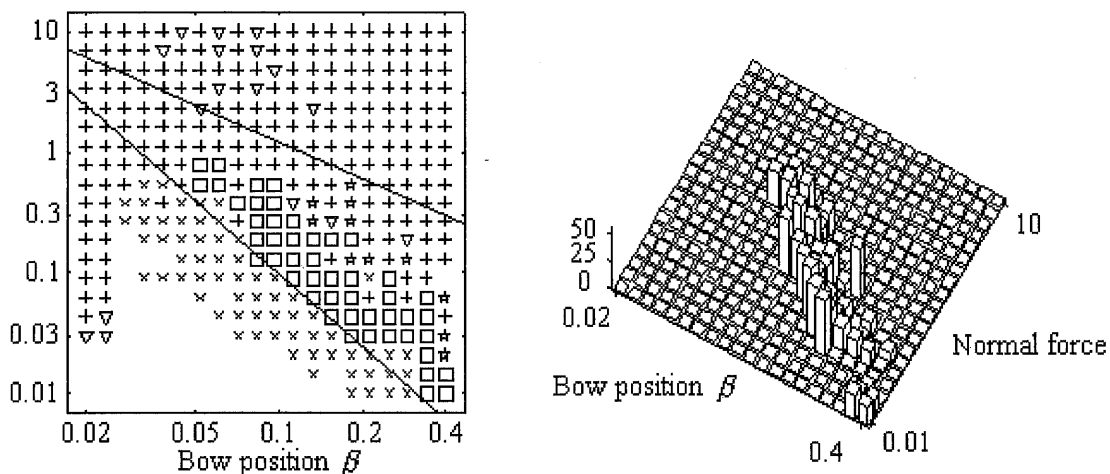


Figure 5. Results of transient bowing simulations using friction-curve model. (a) Schelleng diagram of normal force (N) versus bowing position; (b) transient length in periods.

It is immediately apparent on comparing these figures that the region of Helmholtz motion is significantly bigger for the thermal model — in other words, this model gives a bowed string which is “easier to play” than that using the friction-curve model. The transient lengths tell a similar story. For each value of β , the thermal model shows long transients at the lowest force for which Helmholtz motion occurs, as double-slipping motion takes a long time to give way to Helmholtz motion. For almost all β values the transients shorten rapidly and consistently as force increases. By contrast, the friction-curve model shows generally longer transients and a more irregular pattern which would presumably appear confusingly inconsistent to a player.

Figure 4a and, less clearly, Figure 5a show traces of the wedge-shaped region of Helmholtz motion predicted by Schelleng. Lines are superimposed on the figures, indicating the predicted

slopes of -1 and -2 for the two force limits. The vertical positions of these lines are arbitrarily chosen, near the observed boundaries of Helmholtz motion in Fig. 4a, so that only the slopes of the two lines should be regarded as having any theoretical significance. The differences between the two models are sufficiently striking that it should prove straightforward to determine which is better supported by experimental results. Such a comparison would provide a key piece of evidence for the rival frictional theories.

4. CONCLUSIONS

The context of this paper is that models of the bowed string are reaching a sufficiently sophisticated state that it has become sensible to seek detailed, quantitative agreement with experiment. It has been argued here that the main uncertainty may at present lie in the theoretical description of the frictional force which drives the string. A model in which the friction force is determined by temperature in the contact zone, rather than by sliding speed, has been proposed on the basis of experimental work on a different stick-slip oscillator. Results have been presented here to show some important consequences of this model when it is used in bowed-string simulations. The particular aspect of behaviour highlighted here is the “Schelleng diagram”, the region of steady-bowing parameter space within which a Helmholtz motion is possible.

The main effect noted is that the thermal friction model is more “benign” than the older friction-curve model. Waveforms depend less critically on the precise details of the bowing gesture assumed, the Helmholtz motion of the string is elicited more readily, and the initial transients tend to be shorter and more regular in structure. At least at a qualitative level, this more benign behaviour seems to match the experience of string players better than the more “jumpy” behaviour of the friction-curve model. Whether this impression will be vindicated by quantitative comparisons with experiments remains to be seen.

ACKNOWLEDGEMENTS

It is a pleasure to acknowledge useful discussions on this material with Ken Johnson, Bob Schumacher, Julius Smith, Stefania Serafin and Paul Galluzzo.

REFERENCES

- [1] J. C. Schelleng: “The bowed string and the player”. *J. Acoust. Soc. Am.* **53** (1973) 26–41.
- [2] L. Cremer: *The Physics of the Violin*, MIT Press, Cambridge MA 1985.
- [3] M.E. McIntyre, J. Woodhouse: Fundamentals of bowed-string dynamics. *Acustica* **43** (1979) 93–108.
- [4] M.E. McIntyre, R.T. Schumacher, J. Woodhouse: Aperiodicity in bowed-string motion. *Acustica*. **49** (1981) 13–32.
- [5] J. Woodhouse: On the playability of violins. Part I: reflection functions. *Acustica* **78** (1993) 125–136.
- [6] J. Woodhouse: On the playability of violins. Part II: minimum bow force and transients. *Acustica* **78** (1993) 137–153.
- [7] R. T. Schumacher, J. Woodhouse: Computer modelling of violin playing. *Contemporary Physics* **36** (1995) 79–92.
- [8] J. H. Smith, J. Woodhouse: The tribology of rosin. *J. Mech. Phys. Solids* **48** (2000) 1633–1681.
- [9] J. Woodhouse, R. T. Schumacher, S. Garoff: Reconstruction of bowing point friction force in a bowed string. *J. Acoust. Soc. Amer.* **108** (2000) 357–368.

- [10] M. E. McIntyre, R. T. Schumacher, J. Woodhouse: On the oscillations of musical instruments. *J. Acoust. Soc. Amer.* **74** (1983) 1325-1345.
- [11] J. Woodhouse, A. R. Loach: The torsional behaviour of cello strings. *Acustica — acta acustica* **85** (1999) 734–740.
- [12] F. G. Friedlander: On the oscillations of the bowed string. *Proc. Cambridge Phil. Soc.* **49** (1953) 516–530.

